Structure evolution and phase transition in odd-mass nuclei

D. Bucurescu and N. V. Zamfir
Horia Hulubei National Institute for Physics and Nuclear Engineering, P.O.B. MG-6, 077125 Bucharest-Măgurele, Romania
(Received 16 September 2016; revised manuscript received 28 November 2016; published 30 January 2017)

The evolution of level structures due to the unique parity orbitals $g_{9/2}$, $h_{11/2}$, and $i_{13/2}$ in odd-mass nuclei from Zn to Am is studied within a unified framework, by correlations between ratios of excitation energies in both odd-mass nuclei and their even-even core nuclei. These plots reveal regularities that can be understood in terms of the particle-plus-rotor model, as evolutions along its three limiting coupling schemes: weak coupling, decoupling, and strong coupling, and transitions between them. Peculiar transitions between the decoupling and strong coupling schemes are found in both $i_{13/2}$ structures of neutron-odd nuclei and $h_{11/2}$ structures of proton-odd nuclei, at neutron numbers around 90 and 70, respectively. These are correlated with the critical shape phase transitions from vibrator to rotor from the even-even nuclei in the same regions and are characterized as critical phase transitions too. This behavior is corroborated with a nonmonotonic behavior of the differential variation of the two-neutron separation energies in the same nuclear regions.

DOI: 10.1103/PhysRevC.95.014329

I. INTRODUCTION

Quantum phase transitions in atomic nuclei were first theoretically discussed more than 30 years ago [1–3]. Their experimental recognition in nuclei at low excitation energies, as being similar to those in condensed matter systems, came later [4,5], as it was expected that due the finite nature of the nuclei and the integer numbers of nucleons, nuclear phase transitions cannot be abrupt. This was made possible by using as an order parameter an empirical structure property, e.g., $E(2_1^+)$, the energy of the first excited 2^+ state in even-even nuclei, which presents an almost continuous variation when taken for many nuclei together, unlike the numbers of protons or neutrons [4]. Many other structure properties, when represented as a function of $E(2_1^+)$ may show phase transition discontinuities at some critical value $E_c(2_1^+)$. Because $E(2_1^+)$ closely reflects the equilibrium configuration (shape) of the nucleus, the phase transitions from different nuclear regions are *shape phase transitions*. Other quantities that can be used as a continuous variable to study the structure evolution are, for example, $R_{4/2}$, the ratio between the excitation energies of the 4^+ and 2^+ yrast states, or nuclear mass or mass-related quantities such as the two-neutron separation energy. A shape phase transition is a property of an entire nuclear region. As an example, even-even nuclei around $N = 90$ were interpreted as entailing two phases (spherical and deformed) which change one into the other in a very narrow energy range around a critical value of $E(2_1^+)$.

Critical shape phase transitions were also discussed theoretically within the interacting boson model (IBM) [6] by introducing classes of symmetries as critical point solutions in addition to the three well-known dynamical symmetries [6] U(5) (spherical nuclei), SU(3) (axially deformed nuclei), and O(6) (γ-soft nuclei): X(5) (for the phase transition between U(5) and SU(3) [7], and E(5) [for the transition between O(6) and SU(3)] [8]. Nuclei empirically representing these critical point symmetries were proposed, e.g., [9–11] for X(5) and [12,13] for E(5).

While the interpretation of the collective structures of even-even nuclei has benefited from such benchmarks, the evolution of odd-mass nuclei is more difficult to characterize due to the diversity of level structures even at low excitations, as determined by many different shell model orbitals spanned by the unpaired nucleon. In this work, the structure evolution of odd-mass nuclei will be investigated by examining correlations between different level structure observables, as well as the variation of the two-neutron separation energies.

II. ODD-MASS NUCLEI EMPIRICAL CORRELATIONS

In spite of their more complicated structure, empirical correlations between structure observables, similar to those for even-even nuclei, can be used if one deals with level structures stemming from *unique parity orbitals* (UPOs). These structures have extremely pure wave functions since the UPO does not mix with other orbitals. The high j purity (j is the UPO spin) is their most relevant property and determines nearly identical effects for any UPO, making it possible to apply the same correlation schemes to different mass regions. Three UPO structures ($1g_{9/2}$, $1h_{11/2}$, and $1i_{13/2}$) have been systematically observed [14] for three major shells covering a large part of the nuclear chart.

By using correlations between excitation energies within UPO quasiband structures some similarities with the even-even nuclei were found: universal anharmonic vibrator (AHV) behavior [15–17], tripartite classification [18], and phase transition [15,17]. This work introduces a general framework which allows an interpretation of the UPO structure evolution over wide regions of the nuclear chart, with emphasis on those undergoing a phase transition.

The structure of odd-mass nuclei at low excitation energy entails the coupling of an odd nucleon to an even-even core. A suitable theoretical framework is the particle-plus-rotor model (PRM) [19], where one or a few valence particles moving in the potential of a deformed inert core are coupled to the rotating core. Because we will use its language, we first present a short review of the PRM (for extended presentations, see [20,21]). We consider the case of one particle coupled to an axially symmetric deformed core. The Hamiltonian has essentially three terms: an intrinsic part (movement of the particle in

the deformed potential of the core), a collective part (the rotation of the inert core), and the Coriolis interaction, which couples the particle degrees of freedom with those of the core. Their relative strengths determine what kind of structure is observed. Three limiting coupling schemes were recognized in real nuclei.

(i) *Weak coupling limit*. Realized for very small core deformations. The particle moves on slightly disturbed spherical shell model levels. The energetically favored states of spin $j, j+2, j+4, \ldots$ have relative spacings similar to those of the ground-state (quasi)band (gsb) $0^+, 2^+, 4^+, \ldots$, of the core. This scheme occurs up to deformations $\beta \approx 0.14$ [20], corresponding to cores with ratios $R_{4/2} = E(4_1^+)/E(2_1^+)$ roughly between 2.0 and 2.2.

(ii) *Strong coupling limit* (or *deformation alignment*). Realized when the Coriolis interaction matrix elements are small compared to the single-particle energy splittings between levels with different Ω (projection of the particle angular momentum $\vec{j}$ on the symmetry axis) values. This situation appears in two cases [20,21]: (a) for large deformations β, roughly for $R_{4/2} \gtrsim 3.0$; (b) for small Coriolis matrix elements. For UPOs (large j values), this happens when the odd nucleon is in high-Ω Nilsson orbitals. In this limit the $\Delta J = 2$ favored (spin $j, j+2, \ldots$) and unfavored (spin $j+1, j+3, \ldots$) sequences merge into a single rotational band with spins increasing by one.

(iii) *Decoupling limit* (or *rotational alignment*). Realized when the Coriolis interaction is strong and cannot be neglected compared to single-particle energy splittings and to rotational energy. For the large-j UPO case this takes place when the unpaired nucleon occupies low-Ω states. The decoupling occurs for a relatively wide range of intermediate deformations (from $\beta \sim 0.14$ to about 0.23 [20]; roughly for $R_{4/2}$ between 2.2 and 2.7), and implies a particle angular momentum aligned with the rotational axis of the core [20–22]. In this coupling scheme the favored states (having maximum alignment of the particle spin to the rotation axis) of spin $j, j+2, \ldots$, have relative energies similar to the gsb of the core, while the unfavored states (with lesser alignment) usually lie at higher energies.

Data on the quasiband structures stemming from three UPO orbitals, $g_{9/2}$, $h_{11/2}$, and $i_{13/2}$, as currently found in the ENSDF and XUNDL databases [14] were collected for about 500 nuclei with $30 \leqslant Z \leqslant 95$. For each UPO of spin j we extracted the excitation energies E^* of the states of spin $j, j+2$, and $j+4$ (from the "favored" sequence) and when available, that of the state of spin $j+1$ (from the "unfavored" sequence). We use excitation energies relative to that of the state of spin j, denoted by $E(j+2), E(j+4), E(j+1)$, with $E(I) = E^*(I) - E^*(j)$. We also define the energy ratios $R_{j+4/j+2} = E(j+4)/E(j+2)$, analogous to $R_{4/2}$ from even-even nuclei, as well as $R_j^s = [E(j+2) - E(j+1)]/E(j+2)$, called the *signature splitting index*, a measure of the relative position of the favored and unfavored states [18]. In the strong coupling limit these ratios have well-defined values: $R_{j+4/j+2} = (4j+10)/(2j+3) \approx 2.29$ (2.333 for $g_{9/2}$, 2.286 for $h_{11/2}$, and 2.25 for $i_{13/2}$), and $R_j^s = (j+2)/(2j+3)$ ($\approx$0.54 for all three UPOs).

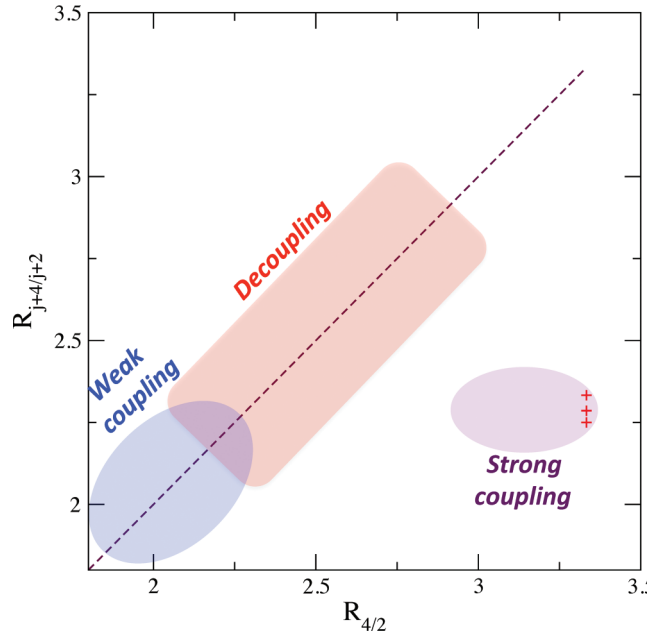

FIG. 1. Colored contours approximately showing the regions where the three coupling schemes of the PRM are expected to occur in the $R_{j+4/j+2}$ vs $R_{4/2}$ representation. Equality of the two quantities is indicated by the dashed line. The three crosses indicate the theoretical limits of the strong coupling for the three UPOs (see discussion in Sec. II).

Because the ratios $R_{4/2}$ in the even-even nuclei directly indicate the degree of collectivity (which is strongly correlated with the number of active particles) and its evolution (precollective nuclei for $R_{4/2} < 2.0$, and collective nuclei from AHV to rotor for $R_{4/2}$ between 2.0 and 3.33), we adopt the correlations between the ratios $R_{j+4/j+2}$ and R_j^s, and $R_{4/2}$ in the core nuclei, as general frameworks to display and discuss the structure evolution in the odd-mass nuclei. The core of an odd nucleus of mass A is defined as its even-even neighbor of mass $A-1$ or $A+1$ if its unpaired nucleon is of a particle or hole nature, respectively. Based on the discussion above, Fig. 1 approximately shows how the three PRM coupling limits are (naively) expected to show up in this type of correlation.

Figure 2 shows the experimental energy ratio correlation for all examined nuclei. Except for some isotopes of In ($Z = 49$) and Sb ($Z = 51$), the precollective nuclei follow the line $R_{j+4/j+2} = R_{4/2}$, in agreement with previous observations concerning the so-called seniority regime, and the similarity between the favored states in the odd-A nuclei and the ground-state quasiband in the neighboring even-even nuclei [18]. The collective nuclei ($R_{4/2} \gtrsim 2.0$) fill up three relatively compact regions, highlighted by the three labeled contours, which form a triangle-like structure. An interesting regularity for the collective nuclei is that the nuclei with odd nucleons of particle (p) type are typically situated in the upper part of the

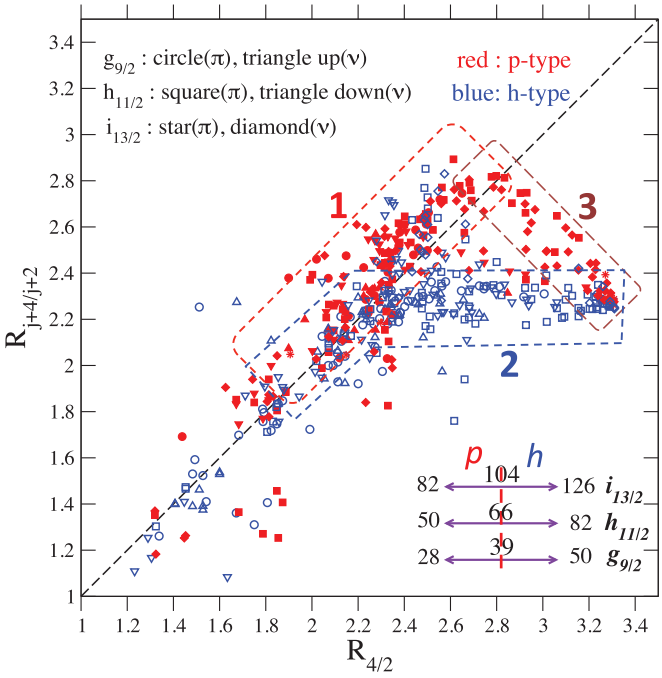

FIG. 2. Correlation between the energy ratios $R_{j+4/j+2}$ of UPO favored sequences and $R_{4/2}$ of the even-even cores. The dashed line indicates equality of the two quantities. The symbols disclose the UPO and the type (proton or neutron, particle or hole type) of the odd particle. See text for the meaning of the numbered contours.

triangle (within contours 1 and 3), while those with hole (h) type in the lower part (within contour 2).

Some of the PRM paradigms are easily noted: weak coupling for the approximately spherical nuclei ($2.0 \lesssim R_{4/2} \lesssim 2.2$), decoupling for some of the transitional nuclei ($2.2 \lesssim R_{4/2} \lesssim 2.7$), and strong coupling for a compact group of many nuclei at $R_{4/2} \approx 3.3$. Other nuclei occupy the lower side (contour 2) and the upper right side (contour 3) of the triangle. The displayed features can be understood on the basis of the PRM structure paradigms (Fig. 1). Around $R_{4/2} \approx 2.0$ all nuclei show, as expected, a weak coupling scheme. At higher $R_{4/2}$ values ($2.2 \lesssim R_{4/2} \lesssim 2.7$), the nuclei with p-type nucleons fill contour 1, which approximately follows the diagonal line (decoupling scheme). This corresponds to the odd particle in Nilsson levels with low Ω, from the first half of the major shell [case (iii) above]. At the largest deformations ($R_{4/2} \approx 3.3$) the nuclei reach the strong coupling limit [case (ii-a)], the compact group of nuclei at $R_{4/2} \approx 3.3$. Contour 3 is an interesting case of rapid transition from decoupling to strong coupling and will be discussed later. Contour 2 is mostly filled by h-particle-type nuclei, comprising nuclei with weak coupling ($R_{j+4/j+2} \approx R_{4/2}$), followed by nuclei characterized by strong coupling ($R_{j+4/j+2} \sim 2.29$). The latter feature is due to the nucleon in the high-j UPO occupying now high-Ω levels in the second half of the shell [small Coriolis interaction, case (ii-b)].

While showing data together for a large number of nuclei (about 500), the correlation plot of Fig. 2 only hints of possible interesting structure evolutions, but does not explicitly disclose how the evolutions of different nuclear regions take place (e.g., the evolution of isotopic chains with the number of

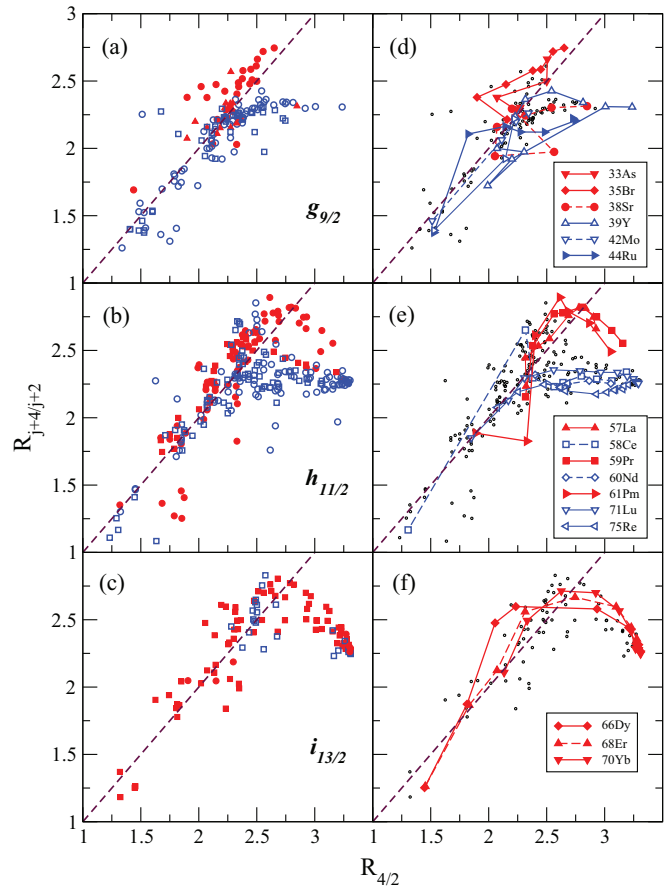

FIG. 3. Panels (a)–(c) are the same as Fig. 1, but separately for each of the three UPOs. Panels (d)–(f) present evolution trajectories of some selected isotopic chains from the respective left-side panels (a)–(c).

neutrons or with the collectivity of the core). Figure 3 repeats the information from Fig. 2, but gives more detail on the nuclear structure evolution. The graphs in Figs. 3(a)–3(c) clearly show that the three considered UPOs behave essentially in the same way. Figures 3(d)–3(f) disclose in each case the behavior of some selected isotopic chains spanning the whole region with available information on the UPO structures. In particular, Figure 3 shows that, within each of the three contours from Fig. 2, isotopes follow evolutions along relatively smooth, similar paths. This observation entitles one to further investigate, in deeper detail, the structure evolution within the contours of Fig. 2. It is also interesting to point out, in Fig. 3(e), the spectacularly different behaviors of, e.g., the proton-odd Pr and neutron-odd Ce isotopes (both having the same even-even Ce cores), or proton-odd Pm and neutron-odd Nd isotopes (with the same even-even Nd cores): with decreasing neutron number, the p-odd nuclei show an evolution along weak coupling and decoupling and then toward strong coupling, while the n-odd nuclei evolve along the weak coupling and strong coupling schemes.

Figure 4 shows the evolution of the signature splitting index R_j^s. Around $R_{4/2} \sim 2.0$, R_j^s is close to zero, corresponding to the weak coupling case. Nuclei from region 1 have negative values, characteristic of decoupling. The h-type nuclei

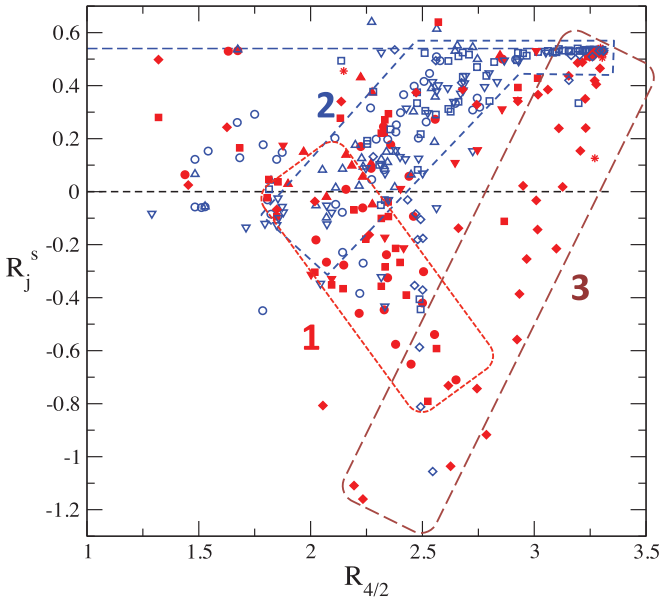

FIG. 4. Similar to Fig. 1, but for the signature splitting index R_j^s (see text). Symbol meanings are as in Fig. 1. The three numbered contours correspond to those from Fig. 1.

(contour 2) have, in general, positive values, characteristic of the strong coupling, with R_j^s increasing from about zero to the strong coupling limit ∼0.54 for $R_{4/2}$ varying roughly between 2.2 and 2.7. Contour 3 shows the rapid transition from decoupling (large negative values) to strong coupling.

Figures 2–4 show some nuclei with h-type nucleon situated within contour 1. They are identified in Fig. 5. The explanation for these "exceptions" is their *oblate* deformation. For oblate

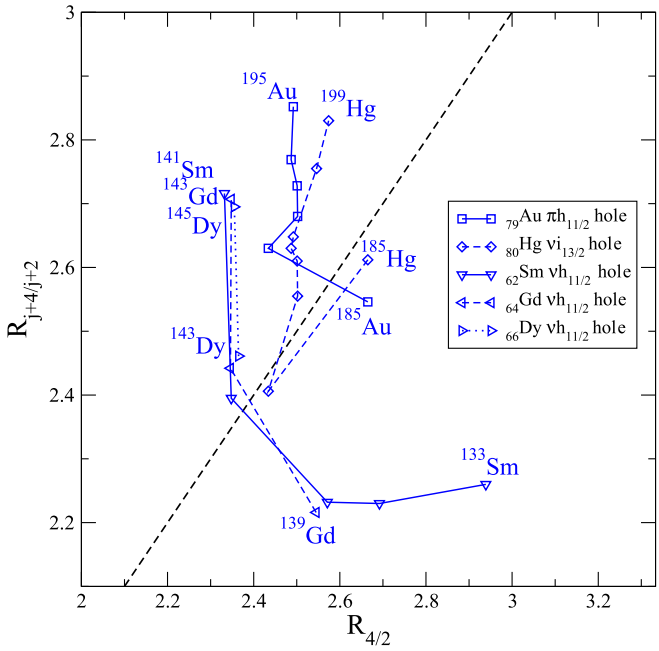

FIG. 5. Detail of Fig. 1 highlighting the nuclei with unpaired hole-type particles which realize a decoupling scheme. For each isotope chain the first and last points are marked with the mass number.

deformation the situation is reversed with respect to that of the nuclei with normal, prolate deformation: the unpaired nucleon is now in low-Ω orbitals, therefore one expects a decoupling scheme [case (iii)]. These nuclei are the following: Au isotopes with masses 185–199 ($\pi h_{11/2}$ structures), all with oblate $11/2^-$ states [24]; Hg isotopes with masses 185–199 ($\nu i_{13/2}$ structures), with oblate $13/2^+$ states [24]; ^{141}Sm ($\nu h_{11/2}$ structure), with an oblate $11/2^-$ state [24]. Due to similarity with their Sm $N = 79$ isotone it is likely that ^{143}Gd and ^{145}Dy have oblate $11/2^-$ states too. All these cases show that the structure of the rotational levels built on high-j orbitals is an excellent tool to distinguish experimentally between prolate and oblate deformations in transitional nuclei [20].

III. PARTICULAR EVOLUTIONS AND SHAPE PHASE TRANSITIONS

We next proceed with a detailed examination of the evolution of isotope chains from the different regions of Figs. 2 and 3. Because the number of nuclei with available UPO structures is larger for the $h_{11/2}$ and $i_{13/2}$ shells, only these cases will be discussed.

A. Shape phase transition in the $\nu i_{13/2}$ structures

The region of transition from decoupling to strong coupling is of special interest. Conventional examination of the energies of favored sequences of isotopic chains compared to those of the gsb of the core nuclei suggests a transition between the two coupling schemes (see, e.g., [21–23]). The present evolution framework highlights a rather interesting situation. In Figs. 2–4 some nuclei follow an evolution along trajectory 3, with a rather rapid transition between the two coupling schemes. The nuclei in this region correspond to two UPOs: $\pi h_{11/2}$ structures in the neutron-deficient La, Pr, and Pm isotopes and $\nu i_{13/2}$ structures in Sm, Gd, Dy, Er, Yb, Hf, and W isotopes.

Figure 6 displays several detailed graphs of the $\nu i_{13/2}$ case, for which the experimental data are especially rich. It contains data for 44 n-odd nuclei with N above 82 (up to 105), from Sm to W. The correlation plots in Figs. 6(a)–6(c) show that all these nuclei evolve along rather compact trajectories. Figure 6(a) shows that the relative energy of the $j + 2$ state $(17/2^+)$ of the favored $\nu i_{13/2}$ structure reaches a minimum value of ∼200 keV at $E_c(2^+) \approx 140$ keV in the core nuclei, which is the critical point of the shape phase transition (from AHV to rotor) from this region [4]. With decreasing $E(2^+)$, the decoupled favored sequence first compresses [$E(j + 2)$ decreases] but, as soon as the core nuclei become deformed it starts to expand rapidly [$E(j + 2)$ increases], evolving toward strong coupling. Figure 6(b) is the analog of the plot $E(4^+)$ versus $E(2^+)$ in even-even nuclei, which disclosed for the first time the *critical* shape phase transition [4]. There is a "turning point" at the minimum value $E_c(j + 2) \approx 200$ keV, which separates the evolution of nuclei having AHV-type cores and decoupling (upper branch) from that of the nuclei with rotor cores quickly approaching the strong coupling (lower branch). Figure 6(c) shows a very compact trajectory of the signature splitting index which also has a turning point at $E_c(j + 2)$, and it is remarkable that it passes through zero value

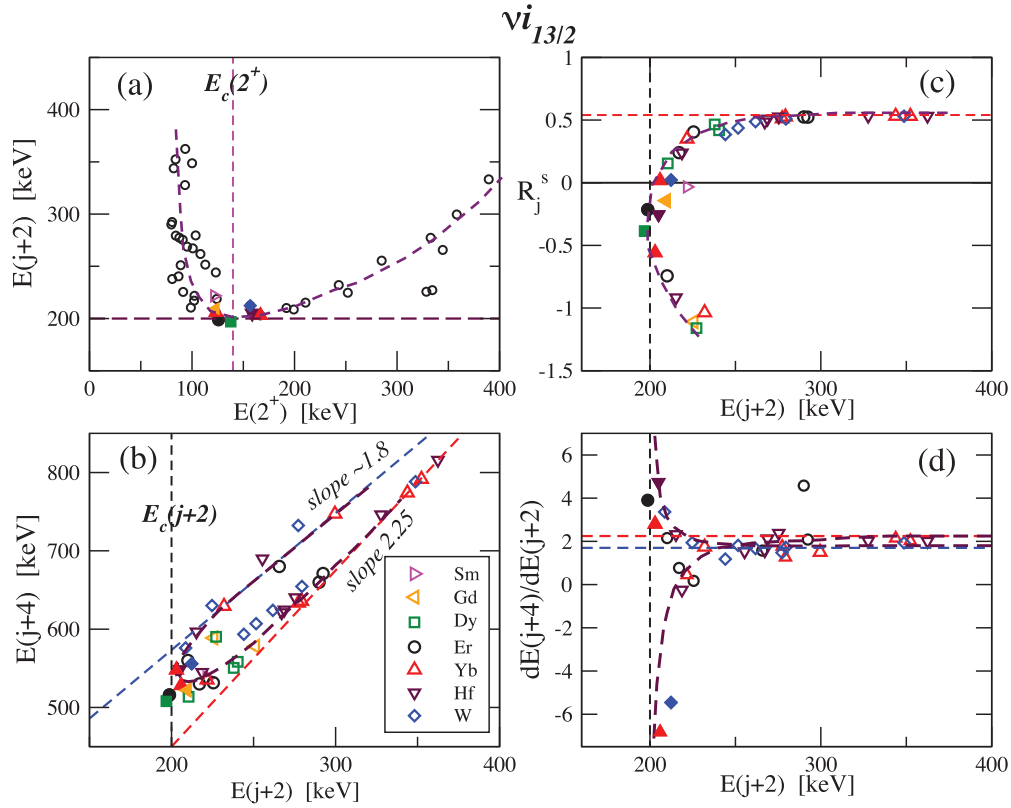

FIG. 6. Different correlations illustrating the critical shape phase transition between the decoupling and strong coupling schemes of $\nu i_{13/2}$ structures (contours 1 and 3; see Figs. 2 and 3). (a) Rapid change of $E(j+2)$ evolution around the value $E_c(2_1^+) \approx 140$ keV corresponding to the X(5) critical point of the core nuclei. (b) Turning point behavior in the $E(j+4)$ vs $E(j+2)$ graph. (c) Evolution of the signature splitting index R_j^s. The dashed lines in (a)–(c) are just drawn through the data points. Filled symbols mark the nuclei closest to the critical point (see text). (d) Derivative of the trajectory from (b) (see text for details).

(where the low-lying favored and unfavored states become degenerate) very close to this turning point. The turning point $E_c(j+2) \approx 200$ keV is a genuine *critical point*, as shown in Fig. 6(d) by the discontinuity in the derivative of the trajectory from Fig. 6(b). The symbols in Fig. 6(d) are values numerically derived for isotopic chains from the points in Fig. 6(b), while the dashed line is the derivative of the continuous empirical curve in Fig. 6(b) drawn through all data points. This derivative is discontinuous at $E_c(j+2) \approx 200$ keV, where it has a vertical asymptote for the two branches.

Seven nuclei closest to $E_c(j+2)$ are highlighted by filled symbols (Fig. 6): ^{155}Gd, ^{157}Dy, ^{161}Er, ^{163,165}Yb, ^{167}Hf, and ^{171}W, while nuclei with $R_j^s \approx 0$ [Fig. 6(d)] are ^{165}Yb, ^{171}W, and ^{153}Sm. Five of these nuclei have cores that fulfill well, or to some extent, X(5) predictions: ^{153}Sm, ^{157}Dy, ^{163}Yb, ^{167}Hf, and ^{171}W, with cores ^{152}Sm, ^{156}Dy, ^{162}Yb, ^{166}Hf, and ^{170}W, respectively [9–11]. Actually, the turning points for the Gd and Er isotopes ^{155}Gd and ^{161}Er have also cores (^{154}Gd and ^{160}Er, respectively) with an yrast band close to the X(5) prediction [10]. Thus, the remarkable behavior of all these isotopic chains around $E_c(j+2) \approx 200$ keV is closely correlated with the X(5) critical point behavior from the core nuclei at neutron numbers between 90 and 96 [10]. Future investigations (both experimental and theoretical) should consider the odd-mass nuclei highlighted above as candidates for empirical representations of the critical point of the transition between the decoupling and strong coupling schemes.

The concept of critical point symmetry was also theoretically developed for odd-mass nuclei. Iachello introduced a critical point Bose-Fermi symmetry called E(5/4) for a $j = 3/2$ particle coupled to an E(5) core [25], which was extended to a multi-j case, $j = 1/2,3/2,5/2$ [the E(5/12) model [26]]. To study the criticality of odd-A nuclei adjacent to even-even nuclei with X(5) symmetry, the X$(5/(2j+1))$ critical point symmetry model was proposed, with a particle in a j orbit coupled to an X(5) core [27]. Some features of the E(5/4) model were approximately recognized in ^{135}Ba [28], and limited agreement with X$(5/(2j+1))$ predictions was found for $j = 1/2$ (^{189}Au), and $j = 5/2$ (^{155}Tb) [27], concluding that the model should be improved by including a multi-orbit scheme. Comparisons of the latter model to the UPO pure-j case were not reported.

Is there any other evidence about the shape phase transitions discussed above? One expects that other structure observables also present an irregular behavior in the region where the shape phase transition takes place. However, for the UPO structures considered above, observables other than level energies (such as electromagnetic transition probabilities) are rather poorly known. To confirm the shape phase transitions by other observations, we resorted to the study of the evolution of the masses of nuclei from the same regions. Nuclear masses

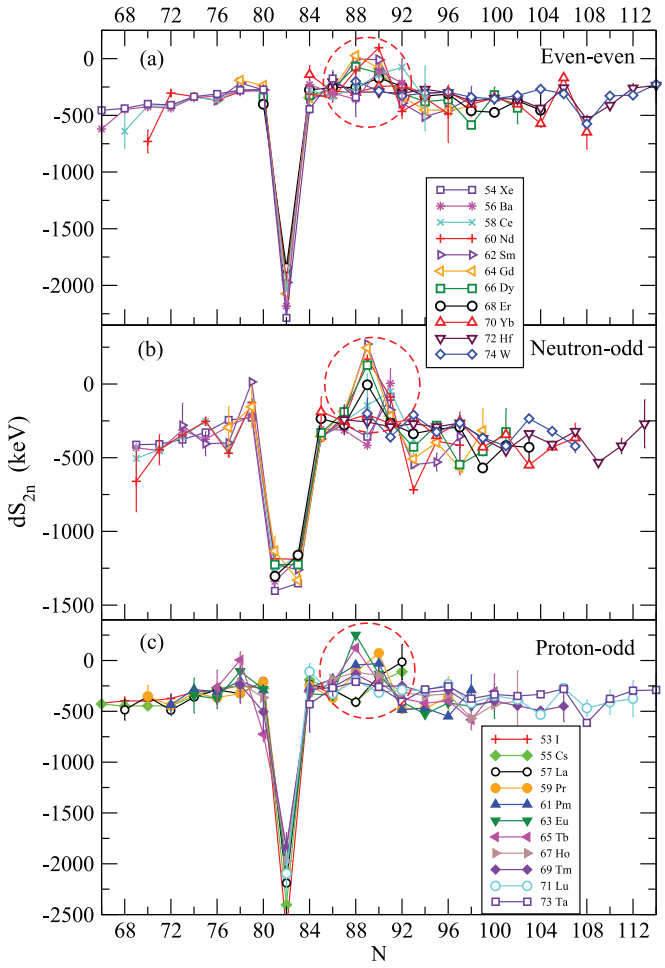

FIG. 7. Evolution of the derivative dS_{2n} of the two-neutron separation energy S_{2n} for (a) even-even nuclei, (b) neutron-odd nuclei, and (c) proton-odd nuclei, respectively, from the $Z = 54$–74 region. The dashed circles indicate the region of shape phase transition at $N \approx 90$ (see text).

contain detailed information on the intrinsic nuclear structure, as determined by the interplay between the average nuclear field and the nucleon-nucleon correlations. The mass-based approach, unlike that following a specific level structure (such as the UPO-based levels), has a more general character. It is well known that different quantities deduced from nuclear masses are rather sensitive to nuclear structure features. Thus, the evolution of the two-neutron separation energy (S_{2n}), when applied to the study of the even-even nuclei, was found useful in disclosing different structure phenomena, like the shell and subshell closures and the shape phase transitions, by nonmonotonic evolutions in certain regions [29]. Especially useful is the differential variation of S_{2n}, defined as $dS_{2n}(Z,N) = [S_{2n}(Z,N+2) - S_{2n}(Z,N)]/2$, which acts as a magnifying glass that better highlights these nonmonotonic behaviors [29].

By using S_{2n} values taken from the 2012 nuclear mass tables [30], we have studied the evolution of dS_{2n} for the odd-mass nuclei in the region where correlation behaviors indicate a phase transition. The results are displayed in Fig. 7. For all nuclei, both even-even and proton-odd or neutron-odd with $Z = 54$–74 and $N = 70$–114, the dS_{2n} quantity presents a rather monotonous evolution with N, around a value of about 500 keV, with two remarkable exceptions. The first is the big negative bump at the magic number $N = 82$, the second is the smaller positive bump around $N \approx 90$. For the even-even nuclei, the latter was associated with the shape phase transition from spherical to deformed nuclei [the X(5) critical point] [29]. The same kind of structure occurs for the odd-mass nuclei [Figs. 7(b) and 7(c)], therefore it can be associated with a shape phase transition phenomenon. In the neutron-odd nuclei this irregularity in dS_{2n} [Fig. 7(b)] confirms the important change of structure shown by the previous results based on the examination of the $\nu i_{13/2}$ UPO structures. Because masses are experimentally known for a larger number of nuclei compared to the cases in which the UPO structures are known, the range of nuclei that can be assigned to phase transition regions is more extended in this case. Thus Fig. 7 indicates that a similar transition takes place in the proton-odd nuclei like the isotopes from La to Eu, in the same range of N values, $N \approx 90$ [Fig. 7(c)]. These neutron-rich odd-mass isotopes are, however, less studied and could not be investigated with the UPO correlation method.

The two approaches discussed so far are somewhat complementary. The one based on the examination of the two-neutron separation energies indicates, through a nonmonotonic evolution, the region where a shape phase transition takes place, whereas by examining correlations of quantities related to UPO excitation energies in odd-mass nuclei one finds the behaviors that characterize the shape phase transition in that region.

B. Shape phase transition in the $\pi h_{11/2}$ structures

Figure 8 presents an analysis, similar to that of Fig. 6, of the transition of $h_{11/2}$ structures in proton-odd nuclei which evolve on trajectories within contours 1 and 3 of Fig. 2 (see also Fig. 3). These nuclei belong to the isotopes Cs to Tb, with N in the range 62–82. The transition toward the strong coupling limit which takes place in neutron-deficient La to Eu isotopes is, in spite of the fact that the data are more incomplete, very similar to that of the $\nu i_{13/2}$ structures. The $E(j+2)$ energy has a minimum at $E_c(2^+) \approx 190$ keV, and a turning point at $E_c(j+2) \approx 235$ keV. The turning points of different isotopic chains approximately correspond to the nuclei ^{125}La (core ^{124}Ba), ^{127}Pr or ^{129}Pr (cores ^{126,128}Ce), ^{133}Pm (core ^{132}Nd), and probably ^{135}Eu (core ^{134}Sm). The corresponding core nuclei, with $N = 68$, 70, and 72, respectively, are among those selected as having yrast state energies close to the X(5) predictions [10]. Nuclear masses in this region are poorly known, therefore examination of Fig. 7 does not offer additional indication about a transition similar to that at $N \approx 90$. We conclude that this transition is, very likely, another critical shape phase transition, corresponding to a spherical to deformed critical shape phase transition in the even-even nuclei from the same region, around $N = 70$.

C. Evolution of the $\pi^{-1} h_{11/2}$ structures

Next we examine a different type of structure evolution, that of the $h_{11/2}$ structures in the proton-hole odd nuclei. These

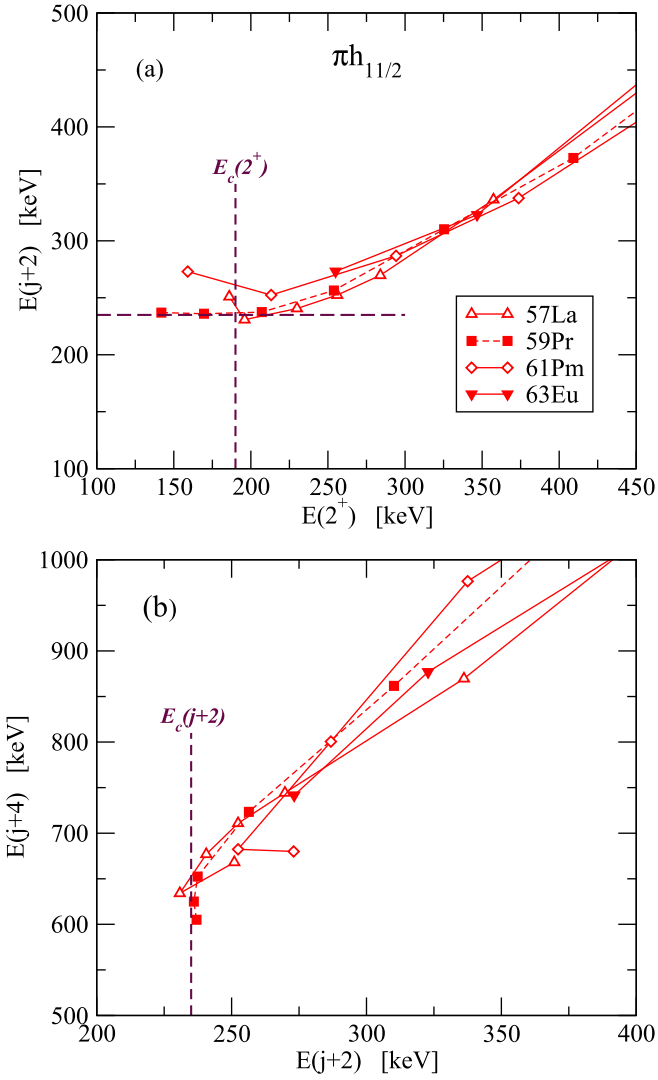

FIG. 8. Similar to Fig. 6, but for the transition region from decoupling to strong coupling [contours 1 and 3 in Fig. 2; see also plots (b) and (e) in Fig. 3] of $\pi h_{11/2}$ structures (nuclei from La to Eu). The analog of Fig. 6(c) is missing here because data on the signature splitting index are too scarce. The nuclei for which $\pi h_{11/2}$ structure data are available (Cs to Tb isotopes) have neutron numbers below 82, the collectivity increasing with decreasing N.

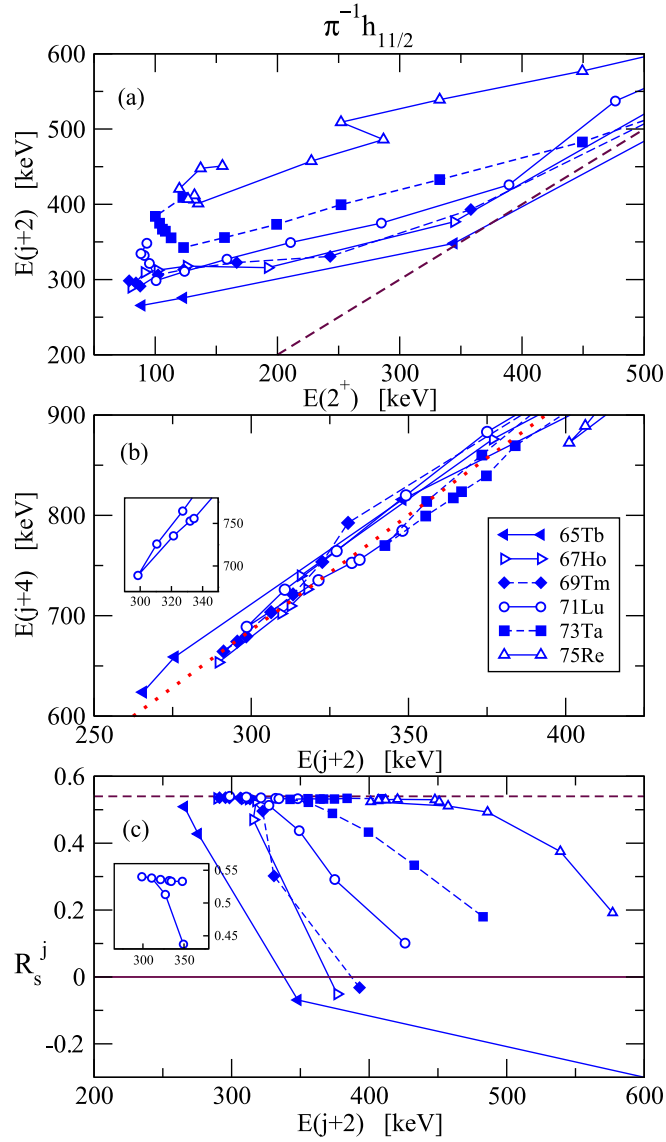

FIG. 9. Similar to Fig. 6, but for $h_{11/2}$ structures of the proton-hole odd-mass nuclei evolving on trajectories within contour 2 in Fig. 2; see also Figs. 3(b) and 3(e). The dashed line in (a) denotes $E(j+2) = E(2^+)$, the dotted line in (b) is for the strong coupling limit $E(j+4) = 2.286E(j+2)$, and the dashed line in (c) is also for the strong coupling limit, $R_s^j = 0.54$. The insets in (b) and (c) show details of the evolution pattern around $N = 98$ of Lu isotopes with N from 88 to 106, which are similar to those of Tm, Ta, and Re isotopes.

comprise nuclei with Z between 65 and 79 and N in the range 82–114. In the graphs of Figs. 2 and 3 these isotopic chains evolve on paths within contour 2. Figure 9 shows graphs analogous to Figs. 6(a)–6(c). As also seen in Figs. 2 and 3, the isotopes with Z between 65 (Tb) and 75 (Re) show first a weak coupling scheme (for the nuclei closer to $N = 82$), then they evolve on trajectories corresponding to strong coupling. The strong coupling is seen in Fig. 9(a) by $E(j+2)$ values larger than $E(2^+)$, in Fig. 9(b) by points which closely follow the strong coupling relation $E(j+4) = 2.286E(j+2)$, and in Fig. 9(c) by values of R_s^j close to 0.54. Figure 9 shows also some peculiarities, which formally resemble those in Figs. 6 and 8. Thus, for the isotopes with Z from 69 to 75, $E(j+2)$ reaches a minimum value [Fig. 9(a)], while in Figs. 9(b) and 9(c) there is a "turning point" behavior. Nevertheless, unlike the case of the shape phase transitions from Figs. 6 and 8, the trajectories for different Z values are similar but do not merge together in a compact path, although they all represent a strong coupling situation. In particular, Fig. 9(c) shows a rather different behavior from that in Fig. 6(c). The origin of the minimum and of the turning points appears to be related to the deformed subshell closure (a gap in the Nilsson level diagram) at $N = 98$; see for example Fig. 8.3 in Ref. [31]. Indeed, the minima in Fig. 9(a) and the turning points in Figs. 9(b) and 9(c) are at $N = 98$ for Ho, Tm, and Lu, and at $N = 100$ for Ta and Re, with nuclei on both sides

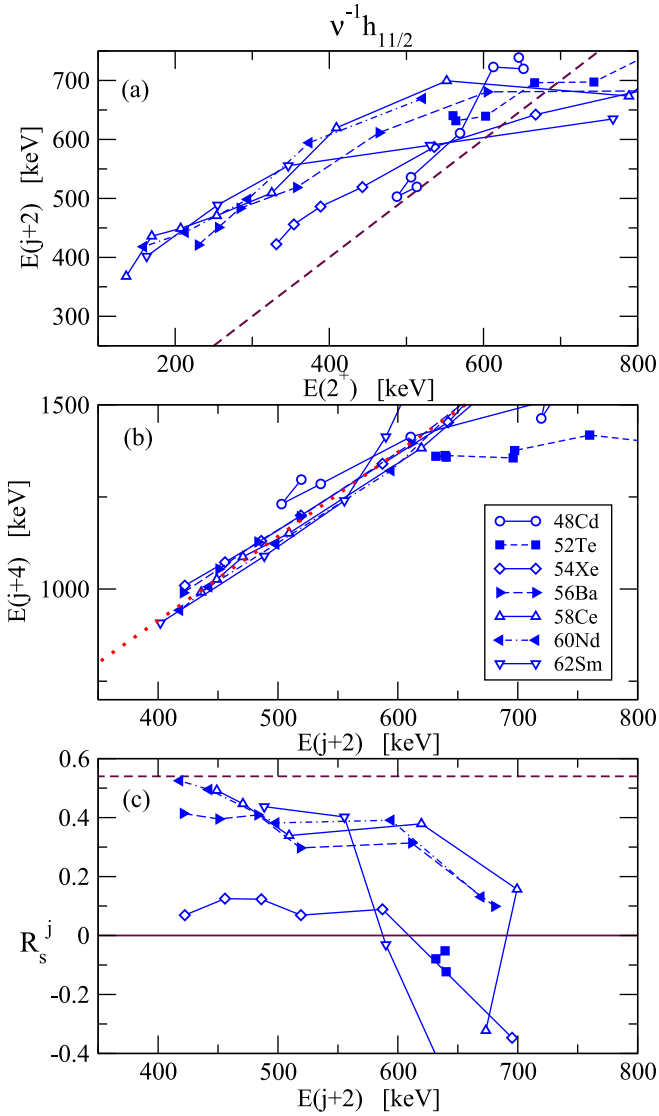

FIG. 10. Same as Fig. 9, but for $h_{11/2}$ structures of the neutron-hole odd-mass nuclei evolving on trajectories within contour 2 in Fig. 2; see also Figs. 3(b) and 3(e).

of these N values being well deformed ($R_{4/2}$ larger than 3.0). The observed behavior may be related to increased rigidity of the deformed nuclei after the additional pairing suppression across the gap at $N = 98$. In Figs. 7(a) and 7(c) there is only a slight hint of the shell gap at $N = 98$, a small negative kink similar to the larger one due to another well-known gap at $N = 108$ [31].

D. Evolution of the $\nu^{-1}h_{11/2}$ structures

The $h_{11/2}$ structures in neutron-hole odd-mass nuclei are known in isotopes from $Z = 44$ (Ru) to $Z = 66$ (Dy) with neutron number N in the range 67–81 (from contour 2). Figure 10 shows the evolution of the chains with the largest number of available UPO structures (Cd to Sm). While Cd, Te, and to a certain extent Xe isotopes display a weak coupling situation (their cores being mostly quasispherical, $R_{4/2} \lesssim 2.3$), the Ba to Sm isotopes show an evolution close to the strong coupling limit, similar to that of the $\pi^{-1}h_{11/2}$ structures (Fig. 9), with the notable absence of the minima and turning points assigned to a deformed shell gap (previous section). The strong coupling limit is reached by only a few Ce and Nd nuclei with well-deformed cores ($R_{4/2} \gtrsim 3.0$), as shown by the signature splitting index [Fig. 10(c)], which also has a different behavior than that in Fig. 6.

IV. CONCLUSIONS

In summary, we have shown that empirical correlations between ratios of relative level energies from the UPO favored and unfavored sequences in odd-mass nuclei and the $R_{4/2}$ ratio in the core nuclei offer an excellent general framework to assess the evolution of these level structures over a large part of the nuclear chart. The three investigated UPOs $g_{9/2}$, $h_{11/2}$, and $i_{13/2}$ behave in a similar way, and isotope chains from different nuclear regions evolve along similar, smooth trajectories. These evolutions, passing through the three limiting coupling cases of the PRM (weak coupling, decoupling, and strong coupling) are remarkably well understood solely based on the type of the unpaired nucleon (particle or hole), without resorting to details of the Nilsson level scheme. The usefulness of these systematics for highlighting nuclei with oblate shape was demonstrated.

Finally, an interesting evolution trajectory was found, making the transition between the decoupling and strong coupling schemes for $\nu i_{13/2}$ structures in nuclei with masses $\sim$150−170 and $N \approx 90$, and for $\pi h_{11/2}$ structures in nuclei with masses $\approx$130 and $N \approx 70$. This transition is correlated to the critical shape phase transition (from vibrator to rotor) of the even-even nuclei from the same regions, and was documented as a critical shape phase transition too. This finding has been corroborated by an independent examination of the evolution of the two-neutron separation energies. Adequate theoretical descriptions of the shape phase transition phenomenon in the odd-mass nuclei, characteristic of coupling a high-j UPO orbital to a transitional core, are expected.

In a very recent work [32], Nomura *et al.* propose an approach to the shape phase transitions in odd-mass nuclei based on theoretical investigations with the energy density functional theory and a particle-plus-boson-core coupling scheme, which is used to define other possible signatures (related to deformations, excitation energies, $E2$ transition rates, and separation energies) of this phenomenon. In particular, they investigate the odd-mass Eu and Sm isotopes with $N \approx 90$ where this shape phase transition takes place. More experimental data, including nonyrast states, are required to better characterize both the nuclear region where this critical shape phase transition takes place (and in particular, the influence of the unpaired particle), and the nuclei that are the best candidates for the realization of the critical point.

ACKNOWLEDGMENT

We acknowledge partial support within the Romanian UEFISCDI Project No. PN-II-ID-PCE-2011-3-0140.

[1] J. N. Ginocchio and M. W. Kirson, Phys. Rev. Lett. **44**, 1744 (1980).
[2] A. E. L. Dieperink, O. Scholten, and F. Iachello, Phys. Rev. Lett. **44**, 1747 (1980).
[3] D. H. Feng, R. Gilmore, and S. R. Deans, Phys. Rev. C **23**, 1254 (1981).
[4] R. F. Casten, N. V. Zamfir, and D. S. Brenner, Phys. Rev. Lett. **71**, 227 (1993).
[5] R. F. Casten, D. Kusnezov, and N. V. Zamfir, Phys. Rev. Lett. **82**, 5000 (1999).
[6] F. Iachello and A. Arima, *The Interacting Boson Model* (Cambridge University, Cambridge, England, 1987).
[7] F. Iachello, Phys. Rev. Lett. **87**, 052502 (2001).
[8] F. Iachello, Phys. Rev. Lett. **85**, 3580 (2000).
[9] R. F. Casten and N. V. Zamfir, Phys. Rev. Lett. **87**, 052503 (2001).
[10] R. M. Clark, M. Cromaz, M. A. Deleplanque, M. Descovich, R. M. Diamond, P. Fallon, R. B. Firestone, I. Y. Lee, A. O. Macchiavelli, H. Mahmud, E. Rodriguez-Vieitez, F. S. Stephens, and D. Ward, Phys. Rev. C **68**, 037301 (2003).
[11] E. A. McCutchan, N. V. Zamfir, R. F. Casten, M. A. Caprio, H. Ai, H. Amro, C. W. Beausang, A. A. Hecht, D. A. Meyer, and J. J. Ressler, Phys. Rev. C **71**, 024309 (2005).
[12] R. F. Casten and N. V. Zamfir, Phys. Rev. Lett. **85**, 3584 (2000).
[13] N. V. Zamfir, M. A. Caprio, R. F. Casten, C. J. Barton, C. W. Beausang, Z. Berant, D. S. Brenner, W. T. Chou, J. R. Cooper, A. A. Hecht, R. Krücken, H. Newman, J. R. Novak, N. Pietralla, A. Wolf, and K. E. Zyromski, Phys. Rev. C **65**, 044325 (2002).
[14] The ENSDF and XUNDL databases, as maintained by the Brookhaven National Laboratories, http://www.nndc.bnl.gov.
[15] D. Bucurescu, G. Căta-Danil, M. Ivaşcu, L. Stroe, and C. A. Ur, Phys. Rev. C **49**, R1759 (1994).
[16] D. Bucurescu, N. Mărginean, I. Căta-Danil, M. Ivaşcu, L. Stroe, and C. A. Ur, Phys. Lett. B **386**, 12 (1996).
[17] D. Bucurescu, N. V. Zamfir, R. F. Casten, and W. T. Chou, Phys. Rev. C **60**, 044303 (1999).
[18] D. Bucurescu, N. V. Zamfir, G. Căta-Danil, M. Ivaşcu, L. Stroe, C. A. Ur, and R. F. Casten, Phys. Lett. B **376**, 1 (1996).
[19] A. Bohr and B. R. Mottelson, Mat. Fys. Medd. Dan. Vid. Selsk **27**, (No. 16) (1953).
[20] P. Ring and P. Schuck, *The Nuclear Many-Body Problem* (Springer-Verlag, New York, 1980), Chap. 3.
[21] R. F. Casten, *Nuclear Structure From a Simple Perspective* (Oxford University, New York, 2000), Chaps. 8 and 9.
[22] F. S. Stephens, Revs. Mod. Phys. **47**, 43 (1975).
[23] R. M. Lieder and H. Ryde, in *Advances in Nuclear Physics*, Vol. 10, edited by M. Baranger and E. Vogt (Springer, New York, 1978), p. 1.
[24] N. J. Stone, Table of nuclear electric quadrupole moments, International Atomic Energy Agency, INDC (NDS)-0650, 2013.
[25] F. Iachello, Phys. Rev. Lett. **95**, 052503 (2005).
[26] C. E. Alonso, J. M. Arias, and A. Vitturi, Phys. Rev. Lett. **98**, 052501 (2007); Phys. Rev. C **75**, 064316 (2007).
[27] Yu. Zhang, Feng Pan, Yu-Xin Liu, Zhang-Feng Hou, and J. P. Draayer, Phys. Rev. C **82**, 034327 (2010).
[28] M. S. Fetea, R. B. Cakirli, R. F. Casten, D. D. Warner, E. A. McCutchan, D. A. Meyer, A. Heinz, H. Ai, G. Gürdal, J. Qian, and R. Winkler, Phys. Rev. C **73**, 051301(R) (2006).
[29] S. Anghel, G. Căta-Danil, and N. V. Zamfir, Romanian J. Phys. **54**, 301 (2009).
[30] M. Wang, G. Audi, A. H. Wapstra, F. G. Kondev, M. MacCormick, X. Xu, and B. Pfeiffer, Chin. Phys. C **36**, 1603 (2012).
[31] S. G. Nilsson and I. Ragnarsson, *Shapes and Shells in Nuclear Structure* (Cambridge University, New York, 1995).
[32] K. Nomura, T. Nicšić, and D. Vretenar, Phys. Rev. C **94**, 064310 (2016).